

## Microstructure and Mechanical Properties of EN AW 6082 Aluminium Alloys after ECAP

### Mikrostruktura a mechanické vlastnosti slitiny hliníku EN AW 6082 po aplikaci ECAP

doc. Ing. Miroslav Greger, CSc.; prof. Ing. Vlastimil Vodárek, CSc.; prof. Ing. Miroslav Kursá, CSc.

VŠB – Technical University of Ostrava, Faculty of Materials Science and Technology, Regional Materials Science and Technology Centre, 17. listopadu 2172/15, 708 00 Ostrava-Poruba, Czech Republic

*Microstructure and texture development of an EN AW6082 alloy during equal channel angular pressing (ECAP) was investigated and correlated with the mechanical properties. The microstructure was effectively refined by ECAP, and the original fibre texture of the extruded aluminium alloy was disintegrated, and a new texture was gradually developed by repetitive ECAP pressing. After 6 ECAP passes following the route B<sub>c</sub>, the elongation was lower than that of the as-extruded aluminium alloy, indicating that the texture softening was dominant over the strengthening due to grain refinement. Cross-section of the original samples was 20 x 20 mm, and their length was 125 mm. Deformation forces were measured during extrusion, resistance to deformation was calculated, and deformation speed was determined approximately. Analysis of structure was made with the use of light microscopy, TEM and SEM. Mechanical properties of the samples after extrusion were determined by tensile test and by the so-called penetration test.*

**Key words:** micro-structures, properties, aluminium alloy, ECAP

*Experimentálně byl ověřován vývoj mikrostruktury slitiny EN AW 6082 při aplikaci extrémní plastické deformace protlačováním úhlovými kanály (ECAP) a stanoven vztah mezi strukturou a mechanickými vlastnostmi. Příčný průřez výchozích vzorků byl 20 x 20 mm, délka vzorků 125 mm. Vzorky byly protlačovány při pokojové teplotě. Pro zvýšení koncentrace a zrovnoměrnění deformace byly vzorky po jednotlivých protlačeních pootočený kolem podélné osy o 90° a znovu protlačovány (cesta B<sub>c</sub>). Při aplikaci extrémní plastické deformace technologií ECAP probíhá intenzivní zjemňování zrna už v počátečních průchodech vzorků maticí, ale deformace je v objemu vzorků nerovnoměrná. Se zvyšujícím se počtem průchodů vzorků maticí je intenzita zjemňování zrna menší, avšak velikost jednotlivých zrn je rovnoměrnější. Jednotlivá zrna jsou přednostně orientována ve směru hlavní deformace. Po šesti průchodech ECAP tažnost slitiny EN AW 6082 klesá, i když zjemnění zrna pokračuje.*

*Při protlačování byly měřeny deformační síly, vypočítány deformační odpory a deformační rychlosti. Rozbor struktury byl proveden pomocí světelné mikroskopie a pomocí TEM a SEM. Mechanické vlastnosti vzorků po protlačování byly stanoveny zkouškou tahem a provedením penetračního testu. Využití extrémní plastické deformace pro zvýšení mechanických vlastností Al slitin je ve stádiu laboratorních zkoušek.*

**Klíčová slova:** struktura; mechanické vlastnosti; slitina hliníku EN AW6082; ECAP

Extrusion by ECAP method enables obtaining of a fine-grained structure in larger volumes. Products made by this technique are characterised by high strength properties (Fig. 1).

The relation between yield stress and grain size is described mathematically by the Hall-Petch equation:

$$\sigma_y = \sigma_o + k d_g^{-1/2}, \quad (1)$$

where  $\sigma_y$  is the yield stress,  $\sigma_o$  is a material's constant for the starting stress of dislocation movement (or the resistance of the lattice to dislocation motion),  $k$  is the strengthening coefficient (a constant unique to each material), and  $d_g$  is the average grain diameter.

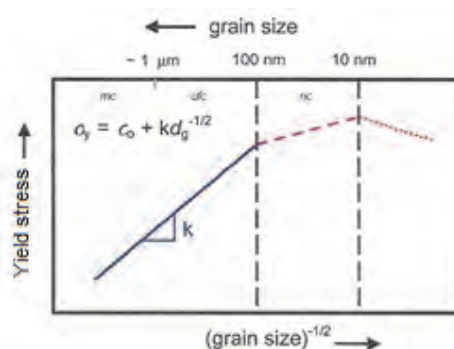


Fig. 1 Schematic representation of the variation of yield stress as a function of grain size in mc, ufc and nc metals and alloys

Obr.1 Závislost meze kluzu na velikosti zrna pro hrubozrnné (mc), ultrajemnozrnné (ufc) a nanostrukturní (nc) materiály

The Hall-Petch relation predicts that as the grain size decreases, the yield stress increases. The Hall-Petch relation was experimentally found to be an effective model for materials with grain sizes ranging from 1 millimetre to 1 micrometre. Consequently, it was believed that if the average grain size was decreased even more to the nanometer length scale, the yield strength would increase as well [1 – 3]. However, experiments on many nano-crystalline materials demonstrated that if the grains reached a size small enough, i.e. the critical grain size, which was typically less than 100 nm, the yield strength would either remain constant or decrease with the decreasing grain size [4 – 6]. This phenomenon has been termed as reverse or inverse Hall-Petch relation. Numerous different mechanisms have been proposed for this relation. As suggested by WITKIN et al. [7], they fall into four categories: (1) Dislocation based (2) Diffusion based (3) Grain boundary shearing based (4) Two phase based. Other explanations, that have been proposed to rationalize the apparent softening of metals with nano-sized grains, include poor sample quality and suppression of dislocation pileups. Many of the early measurements of a reverse Hall-Petch effect were probably the result of unrecognised pores in samples [8, 9]. The presence of voids in nano-crystalline metals would undoubtedly lead to their weaker mechanical properties. The pileup of dislocations at grain boundaries is a hallmark mechanism of the Hall-Petch relationship. However, once grain sizes drop below the equilibrium distance between dislocations, this relationship should no longer be valid [10 – 12]. Nevertheless, it is not entirely clear what exactly the dependence of yield stress should be on grain sizes below this point.

## 1. Development of structure

Influence of the magnitude of plastic deformation on properties of metallic materials is connected with an increase of internal energy. Internal energy increases right to the limit value, which depends on the manner of deformation, purity, grain size, temperature, etc. As a result of non-homogeneity of deformation at the ECAP technique, the internal energy gain differs at different places of the formed alloy. For example, the value of internal energy is different in slip planes, at boundaries and inside cells. It is possible to observe higher internal energy also in proximity of precipitates, segregates and solid structural phases. For usual techniques, pure metals, the medium magnitude of deformation and temperatures, the value of stored energy are said to be approx. around  $10 \text{ J} \cdot \text{mol}^{-1}$  [13 – 16]. At cold extrusion density of dislocations increases with the magnitude of plastic deformation. The density of dislocations depends linearly on the magnitude of plastic deformation in accordance with the well-known equation [17]

$$\rho = \rho_o + K \cdot \varepsilon, \quad (2)$$

where  $\rho_o$  is initial dislocation density ( $10^{10}$  to  $10^{12} \text{ m}^{-2}$ ),  $K$  is a constant,  $\varepsilon$  is the magnitude of deformation.

Flow stress necessary for the continuation of deformation is a function of a number of lattice defects [18]:

$$\tau = \tau_o + k \cdot G \cdot b \cdot \rho^{\frac{1}{2}}, \quad (3)$$

where  $\tau_o$  is initial flow stress,  $k$  is a constant ( $k = 0.3$ ),  $G$  is the modulus of elasticity in shear ( $G_{6082} \sim 25 \text{ GPa}$ ) and  $b$  is Burgers' vector ( $b = 0.3 - 0.4 \text{ nm}$ ).

## 2. Experimental procedure

The objective of experiments consisted in verification of deformation behaviour of the given alloy, determination of resistance to deformation, formability and change of structure at extrusion of alloys. Experiments were made with the use of an apparatus, the diagram of which is shown in Fig. 2. The content of individual elements in the alloy is given in the Tab. 1.

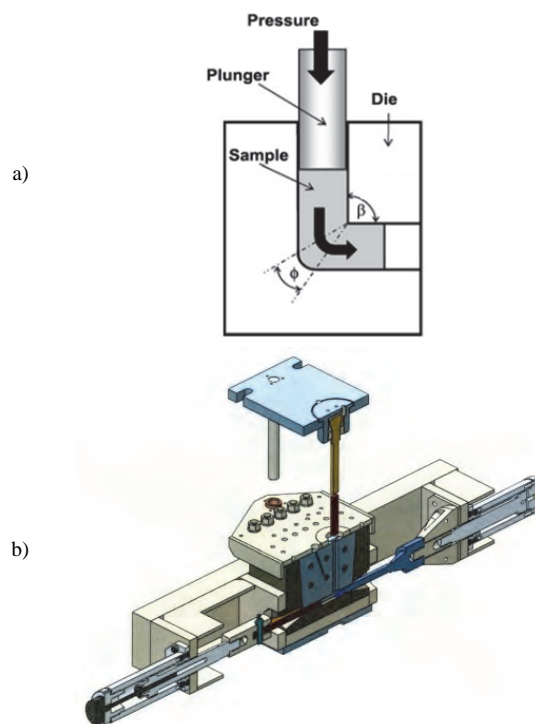


Fig. 2 Schematic illustration of a die used at the present investigation: a) with  $\beta = 90^\circ$  and  $\phi = 20^\circ$ , b) configuration of ECAP workpiece ECAP

Obr. 2 Schématické znázornění tvaru zápustky ECAP: a) s vnitřním úhlem kanálů  $\beta = 90^\circ$  a vnějším úhlem kanálů  $\phi = 20^\circ$ , b) tvar nástrojů ECAP

Tab. 1 Chemical composition of the EN AW 6082 alloy  
Tab. 1 Chemické složení slitiny hliníku EN AW 6082

| Contents of elements | Mg   | Si   | Mn   | Fe   | Cu   | Zn   |
|----------------------|------|------|------|------|------|------|
| (wt. %)              | 1.10 | 0.88 | 0.92 | 0.45 | 0.09 | 0.20 |

During the process, a metal billet is pressed through a die consisting of two channels, equal in cross section and intersecting at an angle  $\beta$ . The billet undergoes essentially simple shear deformation, but it retains the same cross-sectional geometry, so that it is possible to

repeat the pressings for a number of passes, each one refining the grain till the extent, which is determined by the material characteristics.

Deformation forces were measured during extrusion and pressures in the die were calculated. At extrusion with the radius of rounding of edges ( $R_v = 2$  mm;  $R_{vn} = 5$  mm) the pressure in the die varied at the 1<sup>st</sup> pass around  $\tau_{max} = 620$  MPa, and it gradually increased in such a manner that at the fourth pass its magnitude was approximately  $\tau_{max} = 810$  MPa [19]. At extrusion through a die with smaller radii of rounding ( $R_v = 0.5$  mm;  $R_{vn} = 2$  mm) the pressure at the first pass was approx.  $\tau_{max} = 780$  MPa, and at the third pass it was approx.  $\tau_{max} = 1560$  MPa. Significantly higher values of resistance to deformation and strengthening at extrusion are related to the high absolute value of octahedral stress, which either contributes to the more difficult formation of dislocations or decelerates their movement.

Another factor, which influences significantly flow stress and development of microstructure, is the angle  $\Phi$  which is formed by the axis of the vertical and horizontal channel. This angle determines the magnitude of shearing strain in individual passes, and it can be expressed by the relation [20]

$$\gamma = 2 \cotg\left(\frac{\beta}{2}\right). \quad (4)$$

Shearing strain at the angle  $\beta = 90$  achieves the value 2, and normal deformation the value 2.3. Smaller angle  $\beta$  leads to higher shearing stress at each pass. We have checked the size of the angle  $\Phi$  in the range from  $90^\circ$  to  $120^\circ$  with the use of technological route B<sub>C</sub>. We have ascertained, that refining of grains is the most efficient (under the same magnitude of deformation), at the angle of  $90^\circ$ . This is given by the fact that two slip planes in the sample form in this case the angle of  $60^\circ$ . For materials, forming of which is more difficult, it is more advantageous to apply the angle  $\beta = 120^\circ$  together with higher extrusion temperature. It is possible to calculate the magnitude of accumulated deformation from the relation

$$\varepsilon_N = \frac{N}{\sqrt{3}} \left[ 2 \cotg\left(\frac{\beta}{2} + \frac{\phi}{2}\right) + \beta \operatorname{cosec}\left(\frac{\beta}{2} + \frac{\phi}{2}\right) \right], \quad (5)$$

where  $N$  is a number of passes through a die,  $\beta$  is angle channels,  $\phi$  is the additional angle.

After passes, we achieved in the sample magnitude of total accumulated deformation grain size and mechanical properties (Tab. 2).

Tab. 2 Effective strain intensity, grain size and mechanical properties samples after ECAP  
Tab. 2 Intenzita deformace, velikost zrna a mechanické vlastnosti vzorků po jednotlivých průchodech ECAP

| Number of passes | Total strain intensity $\varepsilon$ | Equivalent area reduction | Grain size | 0.2% <i>YS</i> | <i>UTS</i> | $\frac{UTS}{0.2\% YS}$ | Elongation | $\bar{\sigma} = C \cdot \varepsilon^n$ |
|------------------|--------------------------------------|---------------------------|------------|----------------|------------|------------------------|------------|--|
|                  |                                      | (%)                       |            |                |            |                        |            |  |
| 0                | -                                    | -                         | 50         | 120            | 185        | 1.50                   | 15.5       | 175.10                                 |
| 1                | 1.15                                 | 69                        | 3.5        | 190            | 230        | 1.20                   | 8.5        | 179.95                                 |
| 2                | 2.30                                 | 90                        | 2.0        | 217            | 252        | 1.15                   | 7.5        | 206.90                                 |
| 3                | 3.45                                 | 97                        | 1.5        | 230            | 283        | 1.20                   | 6.5        | 224.30                                 |
| 4                | 4.60                                 | 99                        | 1.1        | 250            | 312        | 1.25                   | 6.0        | 237.65                                 |
| 5                | 5.75                                 | 99.8                      | 1.0        | 265            | 325        | 1.25                   | 5.5        | 248.30                                 |
| 6                | 6.90                                 | 99.9                      | 0.9        | 275            | 340        | 1.25                   | 5.5        | 257.50                                 |

### 3. Experimental results and discussion

#### 3.1 Microstructure

Structure of the initial original samples is shown in Fig. 3 and the structure of samples after individual passes is shown in Fig. 4.

The structure contains ordinary inter-metallic phases corresponding to the given composition of the alloy. Average grain size in the transverse direction was determined by quantitative metallography methods, and it varied around  $50 \mu\text{m}$ . Change of shape of the front and rear end of the sample and maintenance of integrity at individual stages of extrusion depend on the level of lubrication and on radii of rounding of edges ( $R_v$ ,  $R_{vn}$ ) of the extruding channel.

After individual passes the accumulation of deformation strengthening occurred, the basis of which was in the

formed sub-structure, which can be seen in Fig. 5 taken by an electron microscope.

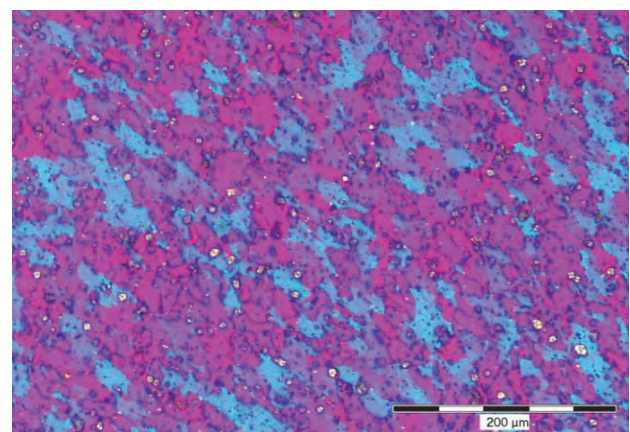


Fig. 3 The microstructure of initial sample of AlSiMg alloy  
Obr. 3 Počáteční mikrostruktura slitiny AlSiMg

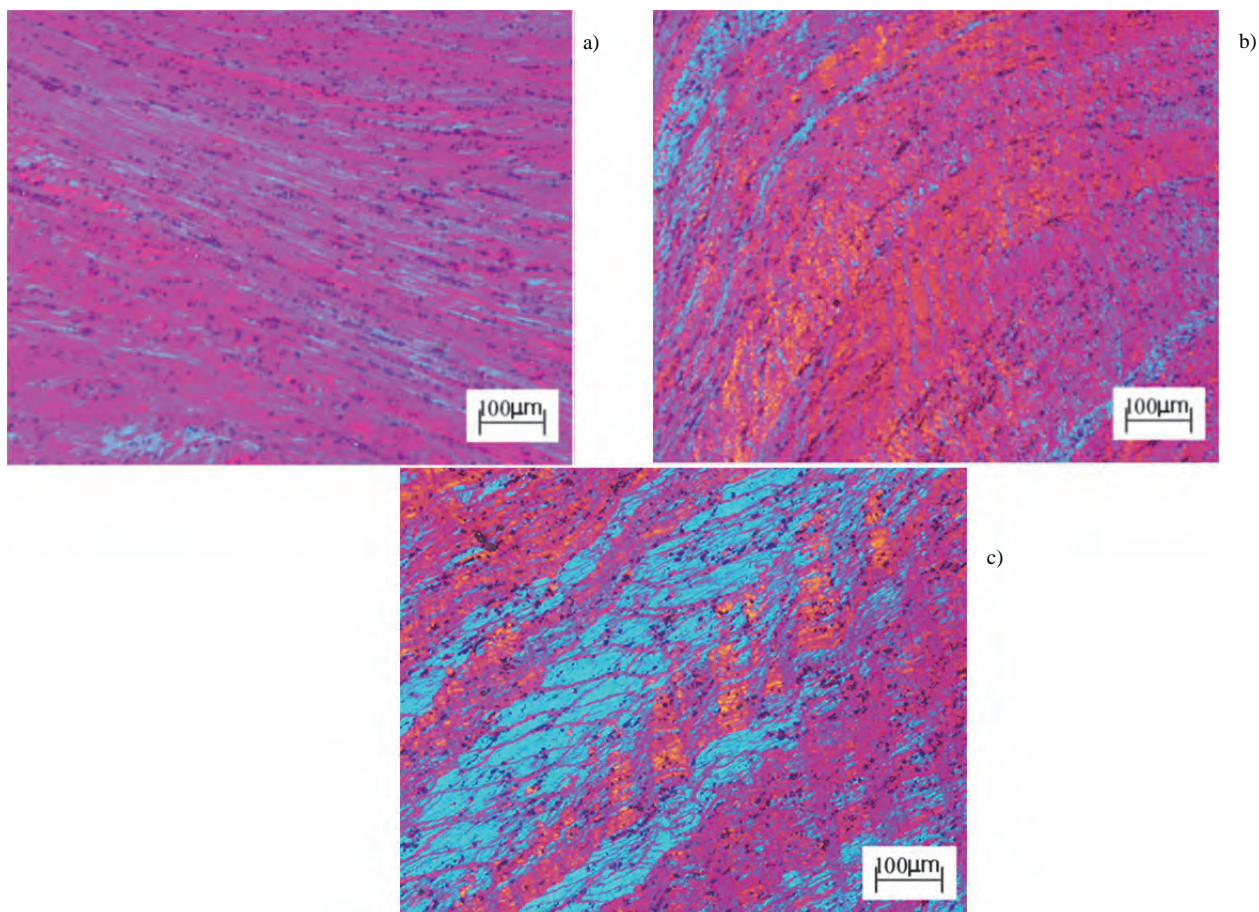


Fig. 4 Microstructure of the samples after ECAP extrusion in longitudinal direction: a) after the 1<sup>st</sup> pass b) after the 2<sup>nd</sup> pass c) after the 3<sup>rd</sup> pass  
Obr. 4 Mikrostruktura vzorků po protlačování ECAP: a) po 1. průchodu, b) po 2. průchodu, c) po 3. průchodu

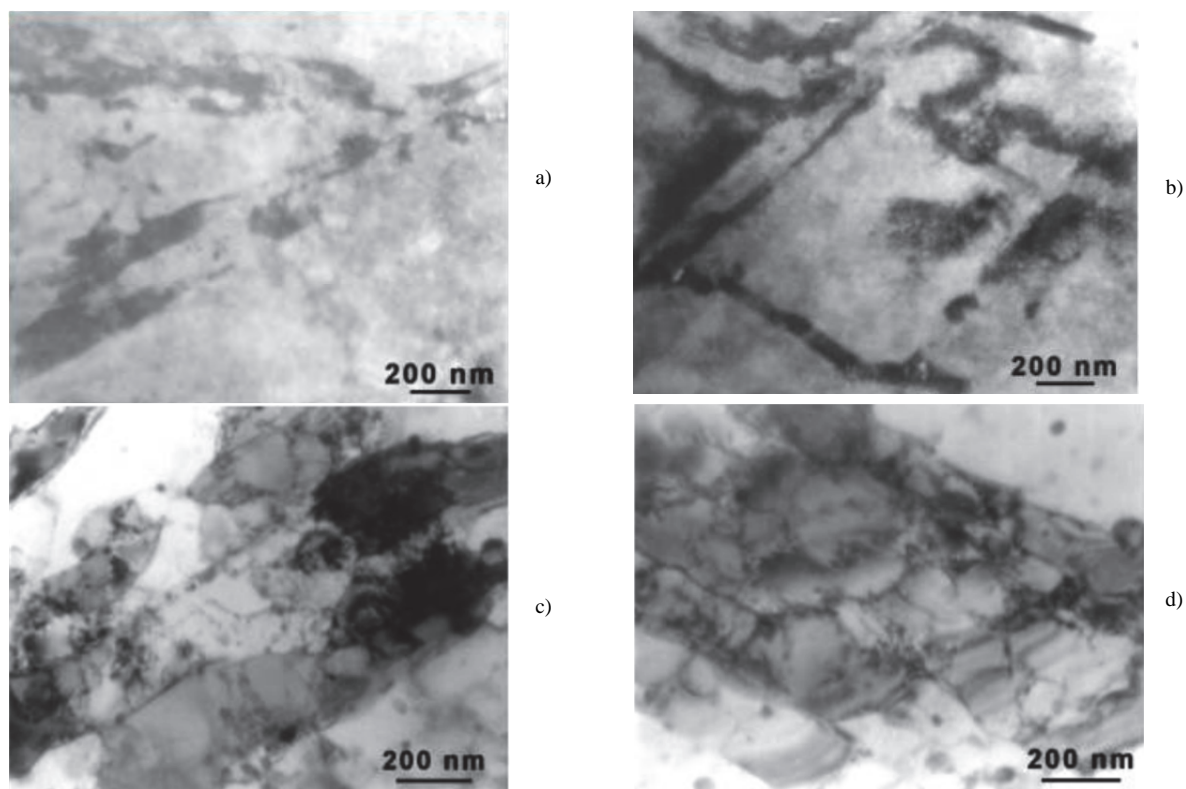


Fig. 5 Sub-structure of AlSiMg alloy after ECAP extrusion: a) after the 1<sup>st</sup> pass, b) after the 2<sup>nd</sup> pass, c) after the 3<sup>rd</sup> pass, d) after the 4<sup>th</sup> pass  
Obr. 5 Substruktura slitiny AlSiMg po prvním až čtvrtém průchodu ECAP

### 3.2 Mechanical properties determined by a tensile test

We have verified the influence of rectangular extrusion on mechanical properties with the use of classical mechanical tensile test [Fig. 6] and the so-called small punch test [21]. After application of the ECAP technique we made from samples miniature test specimens for the tensile test.

Obtained values of tensile strength varied for the aluminium alloy within the range from ultimate tensile strength  $UTS = 185$  to  $340$  MPa. Obtained values of tensile strength correspond very well with the values obtained by simulation and with approximate values based on the results of measurements of hardness. In the frame of evaluation of the influence of the ECAP technique on mechanical properties we have also made tensile tests of investigated materials, but without application of the ECAP technique. We have tested 4 test specimens altogether with a cross-section of  $2.5 \times 5$  mm.

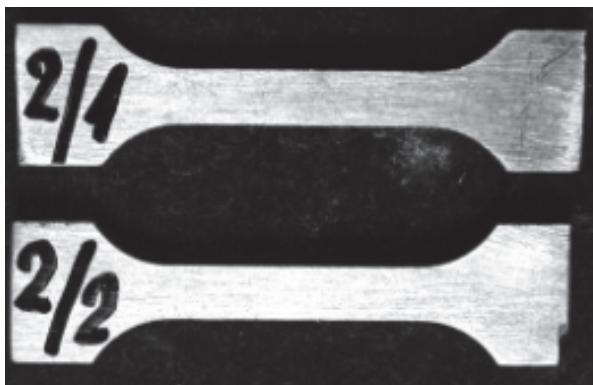


Fig. 6 Form of miniature test specimens for tensile test  
Obr. 6 Tvar vzorků pro tahovou zkoušku

On the basis of the realised experiments, we have determined strength, which, for the AlSiMg alloy, have been found to be  $UTS = 185$  MPa.

As it follows from comparison of strength properties resulting from rectangular extrusion, the strength of the aluminium alloy was increased approximately by 86.5 %. We have performed fractography analyses on broken halves of test specimens. Results of the above-mentioned analyses, including their graphical presentations are given below, Fig.7.

### 3.3 Mechanical properties determined by small punch test

We made from the samples after application of the ECAP technique three test specimens in the form of a disc with a diameter of 8 mm and thickness of 0.5 mm.

Basic mechanical properties were determined on the basis of small punch test, the principle of which consists in penetration of special puncher with the spherical surface through the flat disc-shaped sample, which is fixed between the upper holder and the lower die. On the basis of realised experiments, it is possible to state that tensile strength of the aluminium alloy obtained by small punch test varies in the range from  $UTS = 325$  to  $345$  MPa, which demonstrates very good agreement with the values of tensile strength obtained by the standard tensile test ( $UTS = 335$  to  $340$  MPa).

### 3.4 Analysis of fracture areas in the AlSiMg alloy

Analysis of fracture areas was made with the use of scanning electron microscope JEOL-JSM 5510. From a visual viewpoint, the fracture area looked as planar and fine-grained with indistinctive shear fractures. It was determined by detail micro-fractographical observation that fracture area was formed exclusively by the mechanism of trans-crystalline ductile failure with the morphology of various pits (Fig. 7a). These cavities contained a big number of minuscule particles (Figs. 7b, 7c with marks  $\rightarrow$ ).

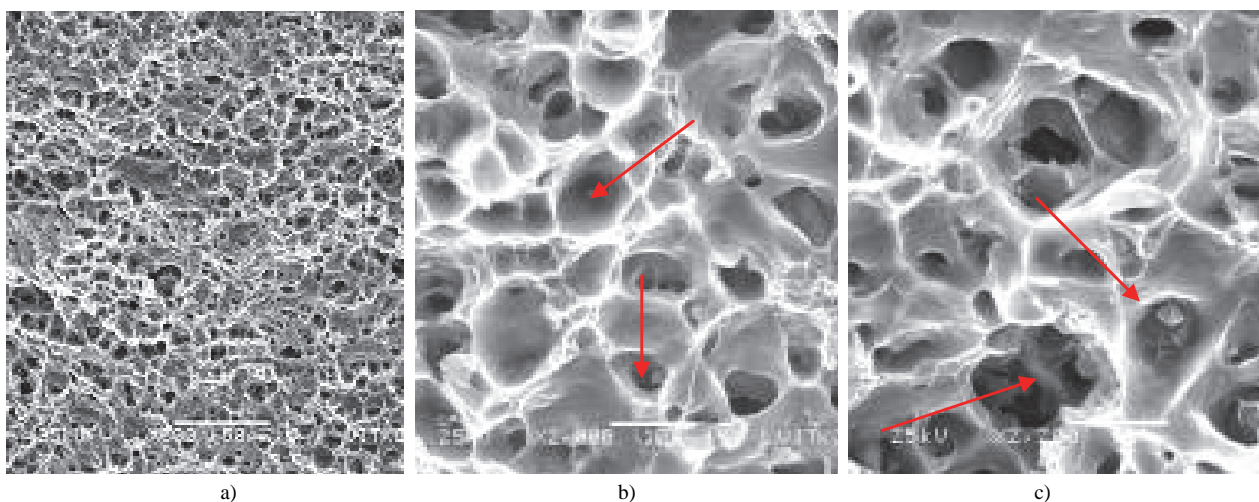


Fig.7 Transcrystalline ductile fracture after ECAP  
Obr. 7 Transkrystalické tvárné porušení po aplikaci ECAP

## Conclusions

We have experimentally verified behaviour of the AlSiMg alloy after extrusion. Method ECAP is a potential tool for refining of grains in poly-crystalline metals. This procedure makes it possible to obtain after 6 passes the grain size of approx. 1  $\mu\text{m}$ . In order to obtain an optimum microstructure, it is necessary to apply more passes with turning of the sample between individual passes by 90° around the longitudinal axis. Development of sub-structure occurs after 4 passes. When the die with the angle of 90° is used, more intensive deformation is achieved, and resistance to deformation is higher than at extrusion with higher angles. Radii of rounding of working edges of extruding channel must correspond to conditions for laminar flow of metal.

## Acknowledgments

This paper was created within the frame of the project No. L01203 "Regional Materials Science and Technology Centre-Feasibility Program" funded by the Ministry of Education Youth and Sports of the Czech Republic.

## References

- [1] VALIEV, R. Z., ZHILYAEV, A. P., LANGDON, T. G. *Bulk Nanostructured Materials: Fundamentals and Applications*; John Wiley & Sons, Inc.: Hoboken, NJ, USA, 2014.
- [2] POKOVÁ, M., CIESLAR, M. Recrystallization of AA3003 Aluminium Alloy after ECAP during Isothermal Annealing. In *METAL 2014*, Brno: Tanger, May 21<sup>st</sup> – 23<sup>rd</sup> 2014.
- [3] JIANG, D., NING, J., SUN, J., HU, Z., HOU, Y. Annealing Behavior of Al-Mg-Mn Alloy Processed by ECAP at Elevated Temperature. *Transaction of Nonferrous Metals Society of China*, 18 (2018) 248-254.
- [4] GREGER, M., KANDER, L., JONŠTA, P., KUŘETOVÁ, B., JÍLEK, L. Development of Fine Grained Structure Using ECAP Technology. In *New Methods of Damage and Failure Analysis of Structural Parts*. Ostrava: VSB-TU Ostrava, 2008, pp. 9–15.
- [5] CABIBBO, M. Microstructure Strengthening Mechanism in Different Equal Channel Angular Pressed Aluminum Alloys. *Materials Science and Engineering A*, 560 (2013) 413-432.
- [6] MURASHKIN, M., SABIROV, I., KAZYKHANOV, V., BOBRUK, E., DUBRAVINA, A., VALIEV, R. Z. Enhanced Mechanical Properties and Electrical Conductivity in Ultra-fine Grained Al Alloy Processed via ECAP-PC. *J. Mater. Sci.*, 48 (2013) 4501–4509.
- [7] WITKIN, D., LEE, Z., RODRIGUEZ, R., NUTT, S., LAVERNIA, E. Al-Mg Alloy Engineered with Bimodal Grain Size for High Strength and Increased Ductility. *Scripta Mater.*, 49 (2003) 4. 297–302.
- [8] GREGER, M., MAŠEK, V. Equal Channel Angular Pressing 6082 Aluminum Alloy. In *COMAT 2012*. Plzeň: Tanger, 2012, pp. 86–90.
- [9] HORITA, Z., FUJINAMI, T., NEMOTO, M., LANGDON, T. G. Improvement of Mechanical Properties for Al Alloys Using Equal-channel Angular Pressing. *Journal of materials Processing Technology*, 117 (2011) 3, 288–292.
- [10] SNOPIŃSKI, P., TAŃSKI, T., KRÓL, M.: Effect of SPD Processing on the Structure and Properties of Al-Mg Alloy. *Inżynieria materiałowa*, 39 (2018) 1, 2–7.
- [11] GREGER, M., KANDER, L., KUŘETOVÁ, B. Plastic Forming of ECAP Processed EN AW 6082 Aluminum Alloy. In *13<sup>th</sup> International Conference on Problems of Material Engineering, Mechanics and Desing*. Trenčín: Trenčianska univerzita, 2008, s. 15–19.
- [12] MURASHKIN, M., MEDVEDEV, A., KAZYKHANOV, V., KROKHIN, A., RAAB, G., ENIKEEV, N., VALIEV, R. Z. Enhanced Mechanical Properties and Electrical Conductivity in Ultrafine-grained Al 6101 Alloy Processed via ECAP-Conform. In *METAL 2015*, Brno: Tanger, 2015, May 3.-5.2015, pp. 2148–2164.
- [13] SHA, G., TUGCU, K., LIAO, X. Z. et al. Strength, Grain Refinement and Solute Nanostructures of an Al-Mg-Si Alloy (AA6060) Processed by High-pressure Torsion. *Acta Mater.*, 63 (2014), 169–179.
- [14] MACKENZIE, P. W. J., LAPOVOK, R. ECAP with Back Pressure for Optimum Strength and Ductility in Aluminium Alloy 6016. Part I: Microstructure. *Acta Mater.*, 58 (2010) 9, 3198–3211.
- [15] GREGER, M., WIDOMSKÁ, M., SNÁŠEL, V., MAŠEK, V. Influence of Microstructures and Mechanical Properties an AlSiMg Alloy after Equal Channel Angular Pressing. In: *ALUMINIUM 2011*, Ústí nad Labem: Univerzita J. E. Purkyně v Ústí nad Labem, 2011, CD-ROM, 6 pp., ISBN 978-80-7414-379-3.
- [16] POKOVÁ, M., ZIMINA, M., CIESLAR, M. The Influence of ECAP on Microstructure Evolution of Aluminium Alloys during In-situ Heating in TEM. *International Journal of Materials Research*, 106 (2015) 7, 676–681.
- [17] SAUVAGE, X., MURASHKIN, M. Y., VALIEV, R. Z. Atomic Scale Investigation of Dynamic Precipitation and Grain Boundary Segregation in a 6061 Aluminium Alloy Nanostructured by ECAP. *Kovové Materialy*, 49 (2011), 11–15.
- [18] ANGELLA, G., BASSANI, P., TUISSI, A., VEDANI, M. Aging Behaviour and Mechanical Properties of a Solution Treated and ECAP Processed 6082 Alloy. *Materials Transactions*, 45 (2004) 7, 2282–2287.
- [19] GREGER, M., WIDOMSKÁ, M. Possibilities of Aluminium Extrusion with Use of an ECAP Method. In: *9<sup>th</sup> International Conference Aluminium in Transport 2003*, Cracow-Tomaszowice: Institute of Non-Ferrous Metals, 2003, pp. 165–169.
- [20] NAKASHIMA, K., HORITA, Z., NEMOTO, M., LANGDON, T. G. Development of a Multi-pass Facility for Equal-channel Angular Pressing to High Strains. *Materials Science and Engineering A*, 281 (2000) 82–87.
- [21] GREGER, M., VODÁREK, V., KANDER, L. Structure and Properties of Materials after Pressing by the ECAP. In *17<sup>th</sup> European Conference on Fracture. Multilevel Approach to Fracture of Materials, Components and Structures*. Brno: VUTIU, The European Structural Integrity Society (ESIS), 2008, pp. 2503–2510.